Chapter 12
Planet Population Synthesis via Pebble Accretion

Bertram Bitsch and Anders Johansen

Abstract The aim of planet population synthesis is to incorporate all physical processes from planet formation theories to arrive at a synthetic population of planets that can be compared to observations. In this way, shortcomings in the theories can be shown. In particular, planet population synthesis has to incorporate theories and models regarding (1) core accretion, (2) gas accretion, (3) planet migration and (4) disk evolution. A general problem of the core accretion scenario is that the building time of a planetary core of a few Earth masses with just the accretion of planetesimals takes longer than the lifetime of the protoplanetary disk. This time-scale problem can be overcome when taking the accretion of pebbles into account. We will review here the differences of planetesimal and pebble accretion on the formation of planets that migrate through evolving protoplanetary disks.

12.1 Introduction

Since the discovery of the first exoplanet a bit more than 20 years ago (Mayor and Queloz 1995), the number of exoplanetary discoveries has risen dramatically. Today, more than 2000 exoplanets are discovered, by various detection methods. These findings included two classes of planets which are not harboured in our own solar system: hot Jupiters and super-Earths (Fig. 12.1). Hot Jupiters are Jupiter sized planets that orbit their host star in just up to a few days, while super-Earths are planets of above two Earth masses, presumably rocky, hence the name. Theories about planet formation have to explain the abundances and frequencies of these discovered planets. Of particular interest is here the population of cold gas giants ($r > 1$ AU) and of super-Earth systems, which are very abundant (Fressin et al. 2013). One way to test the theories is population synthesis, where the available

B. Bitsch (✉) • A. Johansen
Lund Observatory, Department of Astronomy and Theoretical Physics, Lund University, 22100 Lund, Sweden
e-mail: bert@astro.lu.se; anders@astro.lu.se

M. Pessah, O. Gressel (eds.), *Formation, Evolution, and Dynamics of Young Solar Systems*, Astrophysics and Space Science Library 445,
DOI 10.1007/978-3-319-60609-5_12

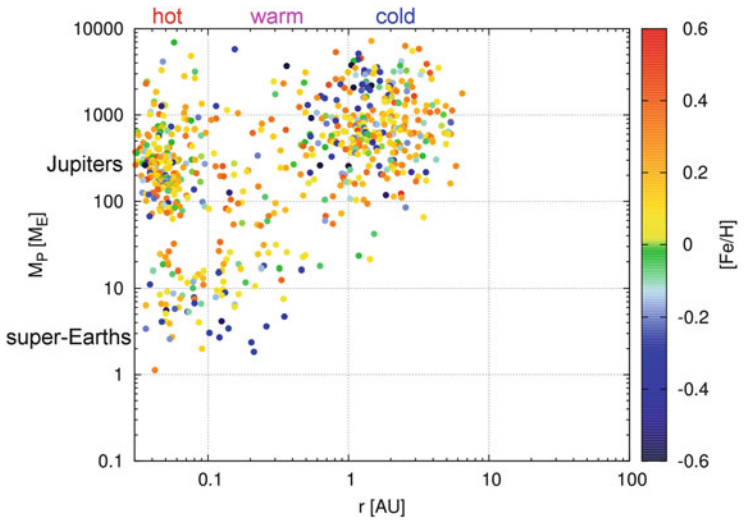

Fig. 12.1 Mass-orbital distance diagram of detected exoplanets either through transits or RV. The *colour coding* gives the metallicity of the planet's host star. Data taken from exoplanets.org

theories of planetary growth and migration as well as disk evolution are combined to synthesise a population of planets. This synthesised population should match the observations in order to confirm the theories of planet formation. If any aspects of the synthesised population does not match observations, theories have to be revised and improved.

The earliest population synthesis simulations pointed out the problem of planetary migration (Alibert et al. 2004; Ida and Lin 2004), namely that type-I migration of low mass planets is way too fast compared to the building time of planetary cores through the accretion of planetesimals. As the planetary core grows in the protoplanetary disk, it interacts with it and moves through it (Ward 1997), where the migration time-scale is much shorter than the lifetime of the protoplanetary disk (Tanaka et al. 2002). This means that planetary cores migrate into the central star before reaching runaway gas accretion, which is when they can potentially open up a gap in the disk that allows the transition into the slower type-II migration regime, potentially saving them from migrating inwards all the way to the star (Baruteau et al. 2014). In order to generate planetary cores that can grow to giant planets at a few AU via gas accretion, planetary type-I migration had to be slowed down by a factor of 100 (Ida and Lin 2004).

Another main problem in the core accretion scenario was the formation of the core itself. In order to form Jupiter's core at 5 AU, the surface density of planetesimals in the protoplanetary disk had to be increased by a factor of $\sim$6 in

order to build big enough cores[1] (Pollack et al. 1996). However, the growth time-scale increases with orbital distance, so forming the cores of Saturn or of the ice giants requires an even larger increase of the solid component of the protoplanetary disk, which is unrealistic.

Here we will show that pebble accretion can help to solve both problems at the same time. Pebble accretion does not only accelerate the growth time-scales of protoplanetary cores, but also allows an efficient formation far away from the central star (Ormel and Klahr 2010; Lambrechts and Johansen 2012). Combining the shorter growth time-scales of pebble accretion-with unreduced planet migration rates, Bitsch et al. (2015b) showed that the formation of giant planets at large orbits is possible in evolving protoplanetary disks. We build on this model and show here the direct comparison with observational data.

This chapter is structured as follows. We first shortly summarise the disk evolution (Sect. 12.2), the planetary growth mechanism via pebble and planetesimal accretion (Sect. 12.3) as well as planet migration (Sect. 12.4). We then combine these things into our population synthesis approach involving pebble accretion and compare these results to core accretion solely by planetesimals (Sect. 12.5). Finally we give a summary in Sect. 12.6.

12.2 Disc Evolution

Inside the disk, dust grains collide and form pebbles (Zsom et al. 2010; Birnstiel et al. 2012; Ros and Johansen 2013) that migrate through the disk due to gas drag (Weidenschilling 1977; Brauer et al. 2008). Clouds of these pebbles can collapse under their own gravity and form planetesimals, aided by the streaming instability (Youdin and Goodman 2005; Johansen and Youdin 2007). These planetesimals can then accrete leftover pebbles and finally form the cores of giant planets (Lambrechts and Johansen 2012), which migrate through the disk (Ward 1997; Paardekooper and Mellema 2006; Kley and Crida 2008; Kley et al. 2009). Even though all these processes happen on different time and length scales, they all strongly depend on the underlying disk structure (temperature T, gas surface density Σ_g, aspect ratio H/r, viscosity ν), making the protoplanetary disk structure a key parameter for understanding planet formation. Every planet formation model is dependent on the underlying disk structure and the results apply only for the assumed disk structure.

One of the most used disk models is the Minimum Mass Solar Nebula (MMSN), which is essentially a power law in surface density and temperature (Weiden-

[1]The main problem here is the planetesimal isolation mass, at which the planet stops growing. It increases with the available amount of planetesimals, Eq. (12.8).

schilling 1977; Hayashi 1981), where the surface density profile is given by

$$\Sigma_{\rm g}(r) = \beta_\Sigma \left(\frac{r}{\rm AU}\right)^{-3/2} . \tag{12.1}$$

The aspect ratio of the disk follows

$$\frac{H}{r} = 0.033 \left(\frac{r}{\rm AU}\right)^{1/4} , \tag{12.2}$$

which indicates that there are no planet traps due to the entropy driven corotation torque, because those traps exist only when H/r decreases with orbital distance (Bitsch et al. 2014). The time evolution of the surface density can be parameterised through

$$\beta_\Sigma = \Sigma_0 \exp\left(\frac{-t}{\tau_{\rm disk}}\right) , \tag{12.3}$$

where $\tau_{\rm disk}$ is the disk's lifetime and $\Sigma_0 = 1700\,{\rm g/cm^3}$.

However, the temperature structure of a protoplanetary disk is much more complex than a simple power law. The temperature structure is given by a balance between viscous and stellar heating with radiative cooling. Viscous heating dominates in the dense inner parts of the protoplanetary disk, while stellar heating dominates the structure of the outer disk. As the disk evolves in time, it loses mass and thus viscous heating becomes less important in the later stages of the disk evolution.

The opacity of the disk $\kappa_{\rm R}$ is of great importance, as it sets the cooling rates of the disk, $D \propto 1/\kappa_{\rm R}$. The opacity is determined mainly by small dust grains, where the exact value of the opacity depends on the grain size and composition as well as on the dust-to-gas ratio (or metallicity $Z_{\rm dust}$). At the water ice line, water ice grains evaporate and can thus not contribute to the opacity any more, resulting in a jump in opacity. This then dramatically changes the disk structure and with it the radial gradients of surface density and temperature in the disk (Bitsch et al. 2014, 2015a; Baillié et al. 2015). These changes of the disk structure have important consequences for the formation of planetesimals and planets as well as on their migration properties, which also scales with the dust-to-gas ratio (Paardekooper et al. 2011; Bitsch et al. 2015b).

In this work, we will also relate on the disk structure model presented by Bitsch et al. (2015a), where also the change of the luminosity of the central star as it evolves is included. This leads to a decrease in stellar heating, resulting a colder disk in the outer regions of the protoplanetary disk as time evolves. We will show the differences in planet population synthesis studies between this disk model and the MMSN. For both disk models we use an α viscosity of 0.0054.

12.3 Planet Growth Mechanisms

After the formation of the planetary core, the planetary envelope can slowly contract until $M_{\rm env} \sim M_{\rm core}$ when runaway gas accretion sets in and the planet becomes a gas giant (Mizuno 1980). Contraction of the envelope and runaway gas accretion requires a solid core of at least a few Earth masses. However, the formation of a planetary core just by planetesimals or planetary embryos can take longer than the lifetime of the protoplanetary disk, if the metallicity is solar (Levison et al. 2010). In recent years new studies of pebble accretion showed that this time-scale problem can be evaded (Ormel and Klahr 2010; Lambrechts and Johansen 2012) and that the formation of planetary cores well within the lifetime of the protoplanetary disk is possible.

The reason why pebble accretion is much more efficient than planetesimal accretion is caused by the fact that pebbles feel gas drag in contrast to planetesimals. Inside the disk a radial gradient in pressure mimics a force that decreases gravity and causes the gas to orbit at a sub-Keplerian speed. The pebbles, on the other hand, do not feel the pressure gradient and want to orbit on a Keplerian speed, where the velocity difference between gas and pebbles acts as a headwind, causing inward drift of the pebbles, known as radial drift.

When planetesimals enter the Hill sphere of the growing planet, they are only accreted to a tiny fraction, while the rest of the planetesimals are scattered away. Pebbles, on the other hand, feel gas drag and lose angular momentum as they drift through the disk. When the pebbles then enter into the Hill sphere and their friction time is shorter than the time to cross the Hill radius, they can be accreted onto the planet. The planet can therefore accrete pebbles from within its entire Hill sphere, enhancing the planetary growth rate by a factor of 100–1000 (Lambrechts and Johansen 2012). Additionally this growth mechanism allows the formation of planetary cores very efficiently at large orbital distances, explaining the growth of the ice giants in our solar system (Lambrechts and Johansen 2014; Lambrechts et al. 2014).

The starting mass of the planetary seeds in our synthesis simulations is the pebble transition mass $M_{\rm t}$, where the bodies start to accrete in the efficient Hill accretion regime [Eq. (12.6)], which is given by

$$M_{\rm t} = \sqrt{\frac{1}{3}} \frac{(\eta v_{\rm K})^3}{G\Omega_{\rm K}} \,, \tag{12.4}$$

where G is the gravitational constant, $v_{\rm K} = \Omega_{\rm K} r$, and

$$\eta = -\frac{1}{2} \left(\frac{H}{r} \right)^2 \frac{\partial \ln P}{\partial \ln r} \,, \tag{12.5}$$

which determines the subkeplerianity of the gas. Here, H/r is the disk's aspect ratio and $\partial \ln P / \partial \ln r$ is the radial pressure gradient in the disk. We use this mass

[Eq. (12.4)] as starting mass also for simulations where the planetary core grows due to the accretion of planetesimals.

We would like to stress here that the pebble transition mass is larger than the typical mass of planetesimals inferred from the streaming instability, which is roughly 100 km (Johansen et al. 2015). These planetesimals can then grow to reach the pebble transition mass via the accretion of pebbles in the inefficient Bondi accretion regime (Lambrechts and Johansen 2012) or by accreting other leftover planetesimals. This growth phase can take up to 1–1.5 Myr, depending on the local disk properties and how many planetesimals formed inside the disk that can accelerate the initial growth process.

Planets at pebble transition mass accrete from the entire Hill sphere at a rate given by (Lambrechts et al. 2014)

$$\dot{M}_{\mathrm{c,\,2D}} = 2 \left(\frac{\tau_{\mathrm{f}}}{0.1} \right)^{2/3} r_{\mathrm{H}} v_{\mathrm{H}} \Sigma_{\mathrm{peb}} \,, \tag{12.6}$$

where τ_{f} is the Stokesnumber of the pebbles, r_{H} is the Hill radius, v_{H} is the Hill speed $r_{\mathrm{H}} \Omega_K$, and Σ_{peb} the surface density of pebbles. However, if the planets are small, their Hill radius can be smaller than the pebble scale height of the disk ($H_{\mathrm{peb}} = H_{\mathrm{g}} \sqrt{\alpha / \tau_{\mathrm{f}}}$), which only allows accretion in the slower 3D regime (Morbidelli et al. 2015). Pebble accretion self-terminates when the planet reaches the so-called pebble isolation mass (Lambrechts et al. 2014)

$$M_{\mathrm{iso}} \approx 20 \left(\frac{H/r}{0.05} \right)^3 \mathrm{M_{Earth}} \,. \tag{12.7}$$

At M_{iso} the planet is massive enough to carve a partial gap in the protoplanetary disk, which is caused by an exchange of angular momentum between the planet and the disk. The disk's material outside of the planetary orbit is accelerated and orbits at a super-Keplerian speed. This means that pebbles entering this region of the disk do not feel a headwind any more, but are accelerated and thus stop drifting inwards. The planet therefore shields itself from pebble accretion. More details on this can be found in Lambrechts et al. (2014) and Bitsch et al. (2015b).

Alternatively, planetary cores can grow via the accretion of planetesimals, which can form in the protoplanetary disk either by the streaming instability (Youdin and Goodman 2005; Johansen and Youdin 2007) or in vortices (Raettig et al. 2015).

In classical models, planets grow through the accretion of planetesimals, where the isolation mass is different compared to pebble accretion. It is given by (Kokubo and Ida 2002; Raymond et al. 2014)

$$M_{\mathrm{iso,pla}} = 0.16 \left(\frac{b}{10 R_{\mathrm{H}}} \right)^{3/2} \left(\frac{\Sigma_{\mathrm{pla}}}{10} \right)^{3/2} \left(\frac{r}{1\mathrm{AU}} \right)^{1.5(2-s_{\mathrm{pla}})} \left(\frac{M_\star}{M_\odot} \right)^{-0.5} \mathrm{M_E} \,, \tag{12.8}$$

where b is the orbital separation of the growing embryos, which we set to $10R_{\rm H}$. Here, $\Sigma_{\rm pla}$ is the surface density in planetesimals, and $s_{\rm pla}$ the negative gradient of the surface density of planetesimals, which we set equal to the gradient in gas surface density.

The accretion rate of planetesimals onto a planetary embryo is set by two different regimes given by planetesimal dynamics: (1) dispersion-dominated growth (Safronov 1969) and (2) shear-dominated growth (Greenberg et al. 1991). In the dispersion dominated regime the scale height of the planetesimal swarm and the approach speed onto the planetary embryo are determined by random velocities $v_{\rm ran}$ that are much larger than the hill speed, $v_{\rm H} = \Omega_{\rm K} R_{\rm H}$. In the shear dominated case, the approach speed $v_{\rm ap}$ is set directly by the Hill speed. These two limits can be combined in the limit of strong gravitational focusing (where $v_{\rm ran} = v_{\rm H}$ and $v_{\rm ap} = v_{\rm H}$) in the following way

$$\dot{M}_{\rm c,plan} = \pi R^2 \Sigma_{\rm pla} \Omega_{\rm K} \frac{6p^{-1}}{\zeta^2} \,, \tag{12.9}$$

where $\zeta = v_{\rm ran}/v_{\rm H}$ determines the accretion regime and $p = R/R_{\rm H}$ is the size of the core relative to its Hill radius. We can rewrite this as

$$p = \frac{R}{R_{\rm H}} = \left(\frac{4\pi G \rho_\bullet}{9\Omega_{\rm K}^2} \right) \,, \tag{12.10}$$

where $\rho_\bullet$ is the density of the planetary core. As a conservative case we set $\zeta = 2$. We assume that all planetesimals form at the time when the disk forms, so that the initial planetesimal distribution in the disk does not change in time as the disk evolves and is therefore solely determined by the initial surface density of planetesimals and thus by the metallicity, where we use $\Sigma_{\rm pla} = Z\Sigma_{\rm g}$.

As the planet stops accreting solids (either planetesimals or pebbles), the planetary envelope can start to cool and contract on a time-scale of several 100 kyrs, as described in Piso and Youdin (2014) and outlined in Bitsch et al. (2015b). As soon as $M_{\rm env} \sim M_{\rm core}$, the envelope contracts rapidly and the planet undergoes runaway gas accretion to form gas giants, where our gas accretion rate is following the simulations of Machida et al. (2010), where the gas accretion rate is directly proportional to the disk's local surface density at the planet's location.

12.4 Planet Migration

Growing protoplanets interact with the surrounding gas and migrate through it. The migration rates are different for low mass planets that are still fully embedded in the disk (type-I migration) and giant planets that open gaps in the disk (type-II migration). The migration rates are obtained in high resolution hydro-simulations including radiation transport for planets in the type-I migration regime (Kley and Crida 2008; Kley et al. 2009; Bitsch and Kley 2011b; Lega et al. 2014, 2015).

However, these simulations are computationally very expensive, especially when long-term evolution of planet(s) are taken into account. Instead the migration rates for low-mass planets in N-body simulations or population synthesis studies are mimicked by fits to hydrodynamical simulations which give the torque acting on embedded planets (Paardekooper et al. 2011). Our simulations contain only single planets, where we assume that their orbit is circular and in mid-plane of the disk. This approach is justified as the disk damps eccentricity and inclination on time-scales much shorter than the migration time-scale for small planets (Bitsch and Kley 2010, 2011a).

The total torque $\Gamma_{\rm tot}$ acting on low mass planets consists of two parts. The Lindblad torque $\Gamma_{\rm L}$ and the corotation torque $\Gamma_{\rm C}$, which arises from the corotation region around the planetary orbit. The total torque is the sum of the two

$$\Gamma_{\rm tot} = \Gamma_{\rm L} + \Gamma_{\rm C} \,. \tag{12.11}$$

The Lindblad torque is caused by spiral waves that are launched by the planet itself. These waves carry away angular momentum from the planet and scale with the radial gradients of surface density, $\Sigma_{\rm g} \propto r^{-s}$, and temperature $T \propto r^{-\beta}$. The Lindblad torque is given in Paardekooper et al. (2011) by

$$\gamma \Gamma_{\rm L}/\Gamma_0 = -2.5 - 1.7\beta + 0.1s \quad \text{and} \quad \Gamma_0 = \left(\frac{q}{h}\right)^2 \Sigma_P r_p^4 \Omega_P^2 \,, \tag{12.12}$$

where q is the mass ratio between planet and star, Σ_P the gas surface density of the disk at the planet's location, and r_P the distance of the planet to the host star. Clearly for normal disk structures, the Lindblad torque is negative and can cause rapid inward migration of planets above one Earth mass, where the migration time-scale is much shorter than the disk's lifetime (Ward 1997; Tanaka et al. 2002).

The corotation torque arises when material that is inside the planetary orbit is deflected by the planet to an exterior orbit, which results in a transfer of angular momentum from the planet to the disk material. Similarly material that is on an exterior orbit of the planet gets deflected inwards and gives angular momentum to the planet. This is the barotropic part of the corotation torque, which strongly depends on the radial gradients in gas surface density.

If there is a radial gradient in entropy, $\xi = \beta - (\gamma - 1.0)s$, where $\gamma = 1.4$ is the adiabatic index in the disk, additional effects come into play. If the disk is hotter interior to the planet and material is deflected outwards by the planet, the material adiabatically expands when embedded in the lower temperature region outside of the planet's orbit. This expansion creates an under-density outside of the planetary orbit. Reciprocally, when material is deflected from the cold outer parts to the inner hot parts of the disk, it adiabatically compresses and generates an over density interior to the planet. The over- and under-density create an additional torque onto the planet, which is the entropy related corotation torque, given by

$$\gamma \Gamma_{\rm C,ent}/\Gamma_0 = 7.9\frac{\xi}{\gamma} \,. \tag{12.13}$$

Outward migration can thus arise in those regions of the disk, where the radial gradients of temperature, surface density, and entropy are steep enough to cause large corotation torques that can overpower the negative Lindblad torque. This normally happens in regions of the disk, where H/r drops radially. In stellar irradiated disks this corresponds to the shadowed regions, which are caused by opacity transitions, for example at the water ice line (Bitsch et al. 2013, 2014; Baillié et al. 2015). Note here that the exact shape of the region of outward migration depends on the jump in opacity, which can change with the total metallicity in dust grains (Bitsch et al. 2015a) and with the chemical composition of the disk (Bitsch and Johansen 2016).

However, the corotation torque is prone to saturation. As the corotation region gives angular momentum to the planet, its own angular momentum decreases and has to be replenished to allow continuous outward migration. This replenishment of angular momentum happens through viscous diffusion of material. We can therefore identify three time-scales that are responsible for outward migration:

- the libration time, which is the time the material needs to make the whole horseshoe turn, given by $\tau_{\rm lib} = 8\pi r_{\rm P}/(3\Omega_{\rm P} x_{\rm s})$, with $x_{\rm s} = 1.16 r_{\rm P}\sqrt{(q/h)}$ being the width of the horseshoe/corotation region
- the U-turn time, which is the time the material needs to make a U-turn close to the planet, given by $\tau_{\text{U-turn}} = h \times \tau_{\rm lib}$
- the viscous time, which is the time the material needs to be replenished in the corotation region, given by $\tau_\nu = x_{\rm s}^2/\nu$, where ν is the viscosity inside the disc

In order to achieve outward migration, the U-turn time has to be smaller than the viscous time, because otherwise the effects of the material transport during the U-turn movement would be washed away. The viscous time also has to be shorter than the libration time, so that the material that is deflected at one side of the planet has replenished its angular momentum when it arrives on the other side of the planet. We can write this as

$$\tau_{\text{U-turn}} < \tau_\nu < \tau_{\rm lib} \,. \tag{12.14}$$

This comparison of time-scales also implies a dependence on planetary mass, which is illustrated in Fig. 12.2.

As the planet grows, it shoves away more and more material from its orbit and carves a gap in the disk, where the planet sits in the middle of it. When the gap becomes deep enough, the corotation region is depleted and the migration rate changes. As the planet feels the torque from both sides of the disk, it stays in the middle of the gap and cannot move with respect to the disk, but only with the disk as it accretes onto the central star. The migration therefore happens on the viscous time-scale of the disk's accretion onto the central star. However, if the planet is much more massive than the gas outside the gap, it will slow down the viscous accretion. This happens if $M_{\rm P} > 4\pi\Sigma_{\rm g} r_{\rm P}^2$, which leads to the migration time scale of

$$\tau_{\rm II} = \tau_\nu \times \max\left(1, \frac{M_{\rm P}}{4\pi\Sigma_{\rm g} r_{\rm P}^2}\right) \,, \tag{12.15}$$

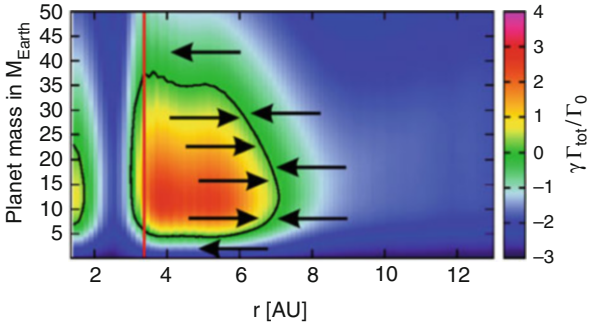

Fig. 12.2 Torque acting on planets as function of planetary mass and orbital distance in the disk model of Bitsch et al. (2015a). *Black contour lines* mark the transition between negative and positive torque, where a positive torque indicates outward migration. This is also indicated by the *thick black arrows*. The radial dependence of the region of outward migration is set by the local gradients in the disk, where the *vertical red line* marks the opacity transition at the water ice line. The upper and lower boundaries are set by torque saturation. Figure from Bitsch et al. (2015a), A&A, 575, A28, 2015, reproduced with permission © ESO

resulting in slower inward migration for massive planets (Baruteau et al. 2014). This is the classical type-II migration regime. However, in recent years this time-scale has been debated and new simulations suggest that type-II migration is not linked to the viscous evolution of the disk (Dürmann and Kley 2015). Additionally, the accretion of material during the migration phase of the planet influences the migration rate itself (Dürmann and Kley 2016; Crida and Bitsch 2016), but here we related back to the classical viscous migration rates for type-II migration [Eq. (12.15)].

12.5 Population Synthesis

All found exoplanets orbit around different types of stars, where not only the spectral type of the stars can be different, but also the metallicity of the host star. Additionally, the exact lifetime of the protoplanetary disk in which planets form and the exact birth time of the planetary seed are unknown. On top of that, the initial distribution of the planetary seeds is also not known. In order to get a homogeneous outcome of the simulations one has to assume a randomisation of certain parameters. In particular we will investigate the change of the following parameters on the evolution and growth of planets:

- The lifetime of the disk and the starting time of the planetary seeds, where we assume a median disk lifetime of 3 Myr, with a Gaussian distribution ($\sigma = 0.5$ Myr), where we fix the minimal and maximal lifetime of the disk to 1 and 5 Myr, respectively.

- The metallicity of the disk is also following a Gaussian distribution, where we put the median at [Fe/H] = −0.0625 ($\sigma = 0.23$), which corresponds to the metallicity of stars in the RV survey of Mayor et al. (2011) to which we compare our simulations.
- For the initial distribution of the planetary seed we assume a linear and a logarithmic distribution in semi-major axis in the regime of [0.1:50] AU.

In the following, we will discuss the influence of the disk's lifetime and of the disk's metallicity on planet growth. We will then put the results together and discuss the differences between the pebble accretion scenario and the growth via planetesimals.

12.5.1 Disc Lifetime

The lifetime of the protoplanetary disk is roughly a few Myr (Mamajek 2009), in which the evolution from planetary seeds to gas giants has to be completed. However, the exact lifetime of a protoplanetary disk is not exactly known and can vary due to external evaporation, cluster environments, and different viscosities inside the disk. Our mean lifetime of the protoplanetary disk is 3 Myr, with a σ of 0.5 Myr, where we limit the maximal lifetime to 5 Myr. Note that the evolution of the accretion rate in time is fixed and does not vary with the disk lifetime. This means that disks with shorter lifetime dissipate at higher accretion rates than disks with longer lifetime. A planetary seeds that forms in the disk, grows and migrates through it. The growth and migration rates are functions of the local disk properties [Eqs. (12.6) and (12.12)], indicating that the exact time when a planetary seed forms in the disk becomes very important.

In Fig. 12.3 we show the evolution of planetary seeds in so-called growth tracks, which show the planetary evolution in mass (via accretion of pebbles and gas) and semi-major axis. Here we have used $Z_{\rm dust} = 0.15\%$ and $Z_{\rm peb} = 1.35\%$, which corresponds to $Z_{\rm tot} = 1.5\%$, corresponding to [Fe/H]$= 0$ and solar value. In Fig. 12.3 the planetary seeds start in a disk that is already 2 Myr old. If the disk's lifetime were only 3 Myr, their final position in the planetary mass-orbital distance diagram is indicated by the black circles, while their final position in a disk that were to live 5 Myr is indicated by the black square. Clearly a longer disk lifetime allows for further growth and migration of already formed cores in the disk. For example, the planetary seed forming at 5 AU only grows to become a super-Earth sized planet if the disk were to live 3 Myr, but can fully contract its envelope and go into runaway gas accretion if the disk lives for a longer time. A longer disk lifetime is also of crucial importance for planetary seeds forming in the outer parts of the protoplanetary disk, as the growth time-scales there are longer.

When comparing Fig. 3 to Fig. 2 of Bitsch et al. (2015b) some clear differences are visible. In particular, in Bitsch et al. (2015b) only one planet migrates all the way to the inner disk before the end of the disk's lifetime at 3 Myr and it is also a giant planet. This difference is due to the change in the disk structure due to the

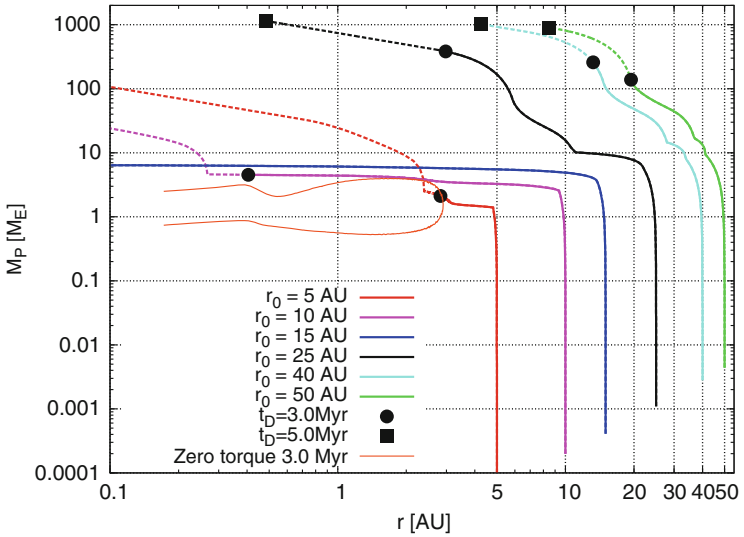

Fig. 12.3 Growth tracks for planets growing via pebble and gas accretion that migrate through the disk, where the planetary seeds start at a disk lifetime of 2 Myr. The *dots* mark the end of the disk's lifetime at 3 Myr, while the *squares* mark the end of the evolution if the disk were to live 5 Myr. Growth tracks that do not feature a circle or a dot reach the inner edge of the disk before the end of the disk's lifetime at 3 or 5 Myr even without being in the gas runaway phase. Note that the planets starting at 10 and 15 AU migrate inwards above the region of outward migration. Clearly a longer lifetime results in an enhanced growth and migration of the planet. Adapted from Bitsch et al. (2015b)

lower metallicity of micro metre sized dust grains, which results in a cooler disk with lower aspect ratio H/r. We assume here a low $Z_{\rm dust}$ as this gives a low opacity, resembling a more realistic grain size distribution, where most of the grains are large and thus have a small opacity. This results in a lower pebble isolation mass in Fig. 12.3 compared to Bitsch et al. (2015b), so the planetary core needs a longer time to accrete a gaseous envelope. Additionally, the lower metallicity in dust grains reduces the region of outward migration (Bitsch et al. 2015a), which allows planets to move inwards close to the central star even before they have reached the runaway gas accretion phase. Note here that the planet starting at 10 AU in Fig. 12.3 is just slightly too massive to be contained in the region of outward migration and therefore moves in slower compared to the planet starting at 15 AU, which reaches the inner edge of the disk even before the disk dissipates at 3 Myr.

Additionally, the amount of pebbles is higher here (1.35%) compared to Bitsch et al. (2015b), where $Z_{\rm pev} = 1\%$ was used, which allows here a faster growth of the planetary seeds. In particular, the planetary seeds starting in the outer part of the protoplanetary disk ($r > 40$ AU) can form gas giants well within the lifetime of the protoplanetary disk. This is also aided by the smaller aspect ratio (smaller amount of dust grains result in colder disks), which concentrates the pebbles in the mid-plane of the disk and thus accelerates growth.

This clearly shows that the final planetary mass and orbital position is not only a function of the initial position of the planet, but also of the lifetime of the protoplanetary disk itself. Additionally this shows that the initial time when the planetary seed is formed in the disk is important, see also Fig. 4 in Bitsch et al. (2015b).

12.5.2 Metallicity

The metallicity in the protoplanetary disk gives the ratio of dust to gas, where a value of $Z_{\rm tot} = Z_{\rm dust} + Z_{\rm peb} = 1.5\%$ corresponds to the solar value, [Fe/H]=0. As the planetary growth rate via pebble accretion rate scales directly with the surface density in pebbles, a change in metallicity has a direct influence on the growth rates of planets. In Fig. 12.4 the mass evolution of planetary cores that form in the same disk structure environment, but with different amounts of pebbles is shown. We keep the planets on fixed orbits for this simulations in order to show the effects of different $Z_{\rm peb}$ clearly, without any influence of planet migration, where the planet might migrate into regions where the accretion rates are different.

A larger metallicity results in a faster growth of the planet [Eq. (12.6)]. The planet therefore reaches pebble isolation mass faster (horizontal line in Fig. 12.4), when $Z_{\rm peb}$ is larger. As the disk evolves in time, H/r drops (Bitsch et al. 2015a) and with it the pebble isolation mass, which determines the final core mass. If the planet grows faster (due to high $Z_{\rm peb}$), it can therefore reach a larger pebble isolation mass. This also means that the formation of gas giants is easier in disks with high metallicity, as

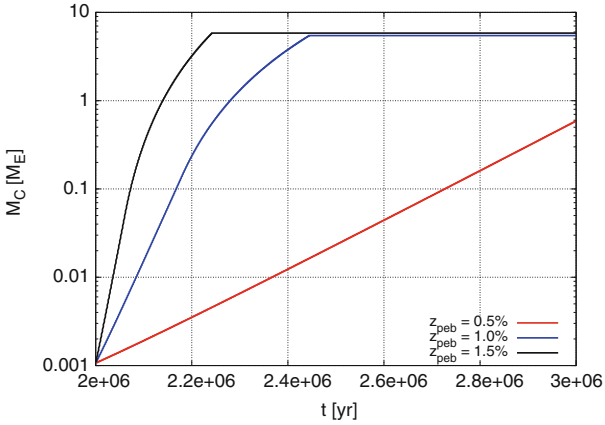

Fig. 12.4 Growth of the planetary core as a function of time for different metallicities in pebbles. Planetary seeds are started at 25 AU and in a disk that is already 2 Myr old. The amount of pebbles $Z_{\rm peb}$ used in Fig. 12.3 is between the *black* and *blue curves*. As the disk evolves in time, the growth rates are not directly proportional to Z any more, as the pebble flux changes in time

larger planetary cores are formed, which can contract their envelope on shorter timescales and reach runaway gas accretion well within the lifetime of the protoplanetary disk. This is in agreement with observations (Fischer and Valenti 2005).

This comparison and the results of the previous section show that the metallicity is not only important for the growth of the planetary core, but also for the orbital evolution of the planet, indicating that the metallicity is a key parameter for the formation of planets.

12.5.3 Accretion via Pebbles

When using the (Bitsch et al. 2015a) disk model, we divide the metallicity into a metallicities for the dust grains $Z_{\rm dust}$ (for the disk structure, see Bitsch et al. 2015a) and for the pebbles $Z_{\rm peb}$ for planet growth (Bitsch et al. 2015b). We use in all the following simulations 10% of the total metallicity for the dust grains and 90% for the pebbles. This results in a cold inner disk, because the cooling rates are very high. This low aspect ratio in the inner disk results in a low pebble isolation mass and in a very small region of outward migration, where planetary cores can outgrow the region of outward migration before they reach runaway gas accretion (Bitsch et al. 2015b; Bitsch and Johansen 2016). The value of $Z_{\rm dust}$ is lower than in Bitsch et al. (2015b), because simulations regarding grain growth and fragmentation predict a size distribution where most of the mass of the dust is in larger particles (Birnstiel et al. 2011), which have a lower opacity than micro metre sized grains. When we use the MMSN disk model, we follow the H/r ratio as outlined above and use 90% of the metallicity in pebbles for planet growth and 10% for the dust. Note that the dust grains are also responsible for the cooling rates needed to calculate the migration of planets.

By varying the initial location of the planetary seed, the disk's lifetime and the metallicity as outlined above, we can provide the final mass and orbital distance of the grown planets and compare them to observations. As the planetary mass is crucial to compare, we rely on observational data that were obtained with the radial velocity method, as this method can constrain the planetary mass. In the RV survey of Mayor et al. (2011) 822 stars are observed, which show a planetary rate of 14% for planets with $M\sin(i) > 50 M_{\rm E}$ and for orbital periods smaller than 10 years (corresponding to 4.64 AU). We therefore simulate 822 growth tracks for each set of simulations to allow a direct comparison with observations. Each growth track is stopped when either the disk dissipates at the end of its lifetime, or when the planet reaches the inner edge of the disk at $r_{\rm inner} = 0.04$ AU or grows to 10,000 Earth masses.

In Fig. 12.5 we show our synthesised planet population in the MMSN disk, while Fig. 12.6 shows our synthesised planet population in the (Bitsch et al. 2015a) disk model. In the MMSN, the synthesised planets match very poorly with the RV data. Especially, the population of the hot giant planets is roughly a factor of 10 too massive and only a small amount of cold gas giants is produced. Additionally,

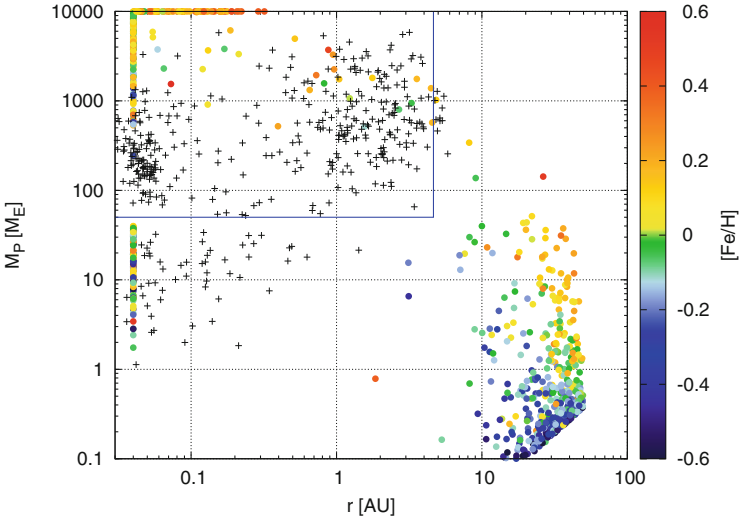

Fig. 12.5 Planet population via pebble accretion in the MMSN disk. The *black crosses* correspond to observations determined through RV measurements, while the *blue box* shows where the RV measurements are complete in the (Mayor et al. 2011) RV survey. The colour scale defines the total metallicity in units of [Fe/H], where 10% of the heavy elements are in micro metre sized dust particles and 90% in pebbles that can be accreted onto the planet

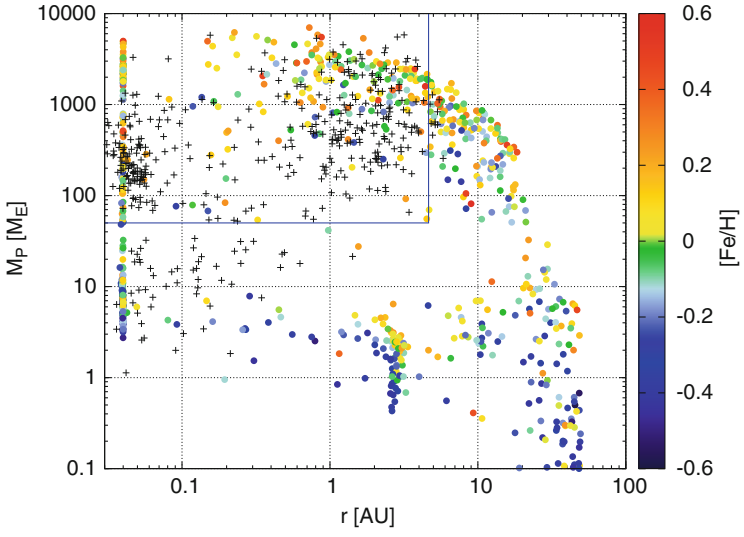

Fig. 12.6 Planet population via pebble accretion in the disk model of Bitsch et al. (2015a). The symbols are the same as in Fig. 12.5

basically no super Earth planets outside of 0.1 AU is formed. Additionally there are 230 planets in the RV box of completeness in the MMSN disk, which corresponds to 26.1%, about a factor of 2 higher than predicted by Mayor et al. (2011). On top of that, the final orbital positions and masses of those planets do not represent the observations at all. In contrast, the synthesis model using the (Bitsch et al. 2015a) disk model shows a better mass distribution for the giant planets and also the formation of super Earths is possible. However, the RV box of completeness shows 271 planets, corresponding to 30.7% which is also a factor of about 2 too high compared to the observations of Mayor et al. (2011).

The reason for the differences of both simulations is the underlying disk model, which significantly differs in the inner regions of the protoplanetary disk (Bitsch et al. 2015a). The MMSN power law disk follows a very steep gradient in surface density towards the inner disk ($\Sigma_g \propto r^{-3/2}$), while the (Bitsch et al. 2015a) model is much shallower ($\Sigma_g \propto r^{-1/2}$), which leads to completely different migration behaviour. In the MMSN disk, only inward migration is possible, while the planets in the (Bitsch et al. 2015a) model can stop their inward migration at the planet trap at the outer edge of the shadowed region caused by the water ice line. As the torque acting on planets also scales directly with the absolute value of the surface density [Eq. (12.12)], the MMSN model features much faster inward migration in the inner regions of the disk. This leads to the increased number of planets of a few to a few 10s of Earth masses at the inner edge of the disk.

As the MMSN disk model features no outward migration, basically no small planets for 1–10 AU are found in Fig. 12.5. The population of super-Earths sitting at a few AU in the (Bitsch et al. 2015a) model is caused by the planet trap at the water ice line. This stops the inward migration of small mass planets and the planets can stay there until the gas disk disappears, if the formation time of the planetary seed is late compared to the lifetime of the protoplanetary disk (see Fig. 12.3).

The gas accretion onto the planetary core is modelled following Machida et al. (2010), where the accretion rate is directly proportional to the gas surface density. This then leads to a much larger accretion rate in the inner disk in the MMSN model, allowing the giant planets to grow to much larger masses as they migrate in the inner disk (within a few AU). However, the masses of the hot gas giants in the inner disk are still larger than the masses of the observed hot Jupiters in the (Bitsch et al. 2015a) disk model.

In the very outer regions of the disk ($r > 10$ AU), the differences in the synthesised planet populations are quite small. This is caused by the fact that the initial growth time-scales via pebble accretion are quite similar in both disks even though the disk models differ in the outer disk. Additionally, all effects mentioned above multiply as the planet growth to become a gas giant, while the growth to an object of just a few Earth masses in the outer disk happens quite locally with only small amounts of planet migration (see Fig. 12.3).

Clearly the structure of the protoplanetary disk is of crucial importance for the outcome of planetary growth simulations, especially in the inner parts of the protoplanetary disk. The MMSN disk totally fails to reproduce either hot Jupiters (with the correct masses) or the super-Earth systems. The (Bitsch et al. 2015a) disk

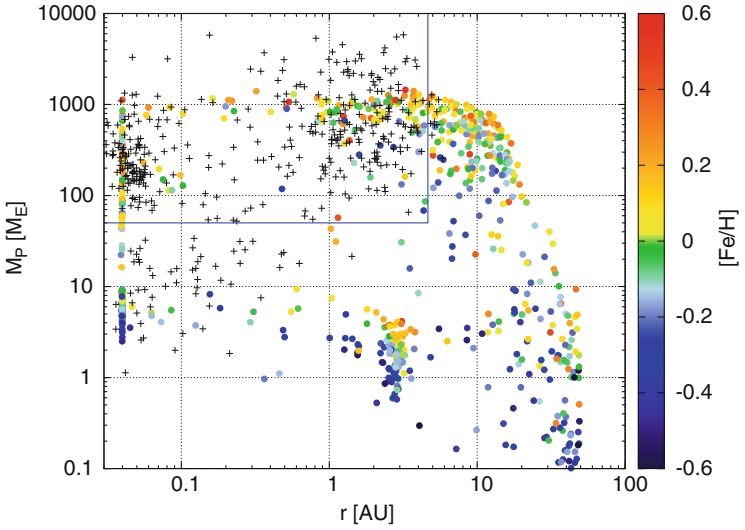

Fig. 12.7 Planet population via pebble accretion in the disk model of Bitsch et al. (2015a), but planetary seeds start only in disks that are already older than 1.5 Myr, otherwise the setup of the simulations is the same as in Fig. 12.6

model allows for a better match regarding giant planets than the MMSN, but even there the population of hot Jupiters is slightly too massive.

The planetary seeds in our simulations start at the pebble transition mass [Eq. (12.4)], which is actually a bit larger than the sizes of planetesimals formed by the streaming instability (Johansen et al. 2015). When these planetesimals are born, they can grow towards the pebble transition mass by accretion of other planetesimals or pebbles in the inefficient Bondi accretion branch (Lambrechts and Johansen 2012), which can take 1–1.5 Myr. In Fig. 12.7 we show the mass-orbital distance diagram, where planetary seeds start in disks that are at least 1.5 Myr old, with a minimal lifetime of 2 Myr. Otherwise the simulations have the same conditions as in Fig. 12.6.

The synthesised hot Jupiter planets match much better with the observations, as the final masses are reproduced very well. In general the final mass of the gas giants is lower, because the planets have less time to accrete a gaseous envelope in the disk. The late formation scenario also populates the parameter space that harbours hot super-Earths better, but inside the RV box of completeness the planetary rate is still about a factor of 1.5 too high (20.2%) compared to Mayor et al. (2011). However, our planets are in single systems (one-planet-per-disk) and we do not take scattering of planets into account, which can easily reduce this number. Also, scattering is an important process to explain the eccentricity distribution of giant planets.

As can be seen in Fig. 12.3, the initial starting position determines the final planetary mass and orbital distance. Therefore, the initial distribution of the planetary seeds in our population synthesis study determines the outcome of our

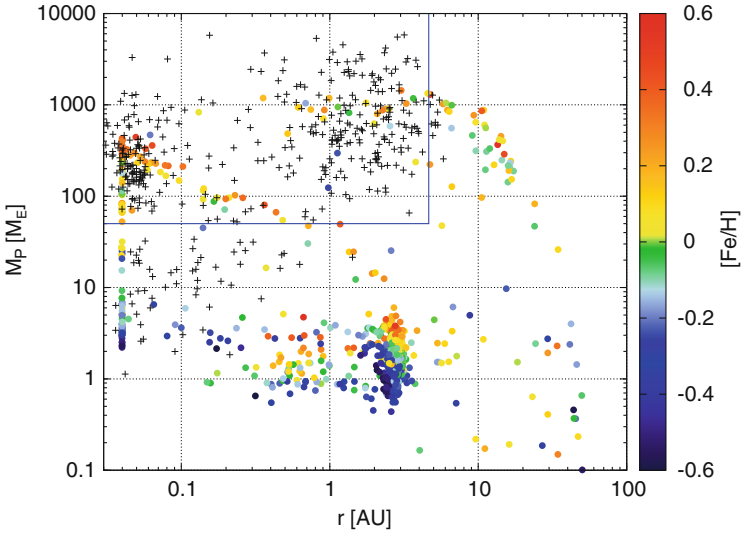

Fig. 12.8 Planet population via pebble accretion in the disk model of Bitsch et al. (2015a), but planetary seeds start only in disks that are older than 1.5 Myr with a logarithmic starting configuration

simulations. The linear starting distribution of planetary seeds as invoked above favours the formation of cold gas giants, as the many planetary seeds start at orbital distances of $r_{\rm init} > 15$ AU. If one were to invoke a logarithmic distribution of the starting location, many more planets form in the inner parts of the disk, where they do not have the chance to grow to become gas giants at wide orbits. We show in Fig. 12.8 the final planetary masses and orbital distances of planetary seeds that formed in a logarithmic starting configuration.

The logarithmic starting configuration of planetary seeds shows less giant planets compared to the linear starting configuration, because planets forming in the inner regions of the protoplanetary disk have a smaller pebble isolation mass and thus a smaller core mass, which makes it harder for those planets to reach the runaway gas accretion phase (Bitsch et al. 2015b). These failed gas giants are left as small rock-dominated planets of orbits of up to a few AU and are much more frequent compared to the results of the linear starting distribution of planetary seeds (Fig. 12.7), where more giant planets form, as giant planets form preferably in the outer disk. In this case, 11.0% of all planets end up in the RV box of completeness defined by Mayor et al. (2011). However, fitting the exact number of Mayor et al. (2011) is only meaningful if multiplicity and scattering are taken into account, which is lacking in our model.

The synthesised planets in Figs. 12.6, 12.7, and 12.8 all share a similar pattern, which is a lack of Neptune mass planets in the inner parts of the disk, which is actually where most of the observed planets in the (Mayor et al. 2011) survey are. The formation of gas giants in our model relies on the planetary seeds reaching

pebble isolation mass so that they can contract their envelope and eventually go into runaway gas accretion. This is limited in the inner disk by the small pebble isolation mass. Small planetary cores therefore stay at the zero-torque position in the inner disk (Fig. 12.3) until they start to undergo runaway gas accretion. This set them all on a very specific type of growth track, as can be seen nicely in Fig. 12.8. This leaves a region of parameter space in planetary mass and orbital distance very void of synthesised planets (10–100 M_E between 0.1 and 1.0 AU). It is very hard to populate this mass bin with planets in simulations, because large planetary cores undergo rapid runaway gas accretion, allowing them to become even larger than 100 M_E within a very short timeframe. This was already noticed in the earliest planet population synthesis studies (Ida and Lin 2004) and identified as a planetary desert.

The formation of these super-Earths and Neptune planets is not entirely understood. In the literature many different ways have been proposed to form these planets (in-situ formation, migration, etc.), but none of the proposed mechanisms seems to satisfy the observational constraints (Ogihara et al. 2015). Additionally, multiplicity is probably a key ingredient needed to form those systems, which is beyond our one-planet-per-disk approach.

12.5.4 Accretion of Planetesimals

We investigate here the growth of planets, where the core builds up by accreting planetesimals. As planets migrate through he disk, they stir up the planetesimals and only a tiny fraction of those are actually accreted onto the planet (Tanaka and Ida 1999). Therefore our planetary seeds grow only until they reach the planetesimal isolation mass, in contrast to previous population synthesis simulations where the planetary seed can additionally accrete up to 100% of the planetesimals that it encounters during its migration (Dittkrist et al. 2014). As soon as the planets reach planetesimal isolation mass, gas accretion can start, which is modelled in the same way as for the pebble accretion simulations.

In Fig. 12.9 we show the orbital distance vs. planetary mass diagram of the growth simulations via planetesimals. Clearly, reaching final masses of above 10 M_{Earth} is very difficult and impossible at orbital distances larger than 1 AU. The reason why planet growth via planetesimals is not successful is twofold. First, the planetary growth rates are slow [Eq. (12.9)] compared to pebble accretion, giving less time to accrete gaseous envelopes after reaching isolation mass. In fact we also integrate 822 growth tracks as in the previous simulations featuring pebble accretion, but out of all these seeds, only $\sim$250 reach a mass larger than 0.1M_E.

Secondly, the planetary cores that are forming suffer from inward type-I migration. As the growth rate is slow, they undergo strong inward type-I migration while still accreting some planetesimals at a low rate and thus cannot accrete a gaseous envelope. They reach the inner regions of the disk before they can start efficient runaway gas accretion and open a gap in the protoplanetary disk, where type-II migration could potentially save them from migrating all the way towards the inner

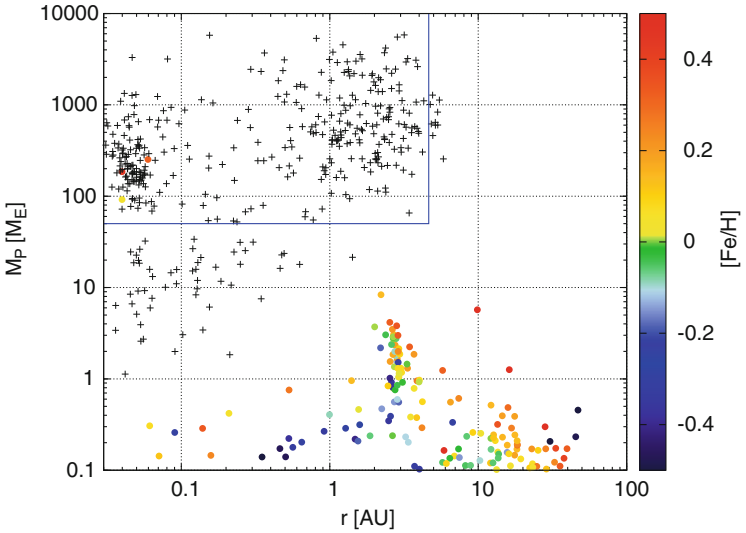

Fig. 12.9 Mass-orbital distance diagram of 822 planetary seeds growing by planetesimal accretion, where only 250 of these seeds grow above M_E. The *colour coding* shows the metallicity for each planet growth simulation. Forming gas giants outside of 0.1 AU is basically not possible

edge. This is consistent with the findings of Ida and Lin (2004) and Alibert et al. (2004) who suggested that planet migration is too fast to form giant planet cores in the planetesimal accretion scenario. The reason why recent population synthesis simulations are successful in producing giant planets is then caused by the different accretion scheme of solids, where the migrating planetary seeds can accrete up to 100% of all leftover planetesimals allowing faster growth (Dittkrist et al. 2014) and by using largely super-solar metallicities.

To overcome the problem of strong inward migration in the type-I migration regime, Coleman and Nelson (2016) invoked the formation of planetary seeds in zonal flows at distances of up to 30 AU from the central star, where the planets can grow without migrating and are then just released when they become massive enough to open up gaps in the disk. In this way the observed giant planet population can be matched. Another approach in overcoming the strong inward migration is to accelerate the growth rates of planets by increasing the amount of planetesimals in the disk, which is taken in recent population synthesis simulations.

We show the results of both approaches in Fig. 12.10, where the left panel shows the mass-orbital distance diagram of planetary seeds growing via planetesimal accretion, but with suppressing all planetary migration, while the right panel shows the mass-orbital distance diagram of planetary seeds growing via planetesimal accretion, where the planetesimal surface density $\Sigma_{\rm pla}$ has been increased by a factor of 10 and planetary migration is taken into account.

When suppressing planetary migration, the final mass of the planet is solely determined by the planetesimal isolation mass and by the time the planet has to

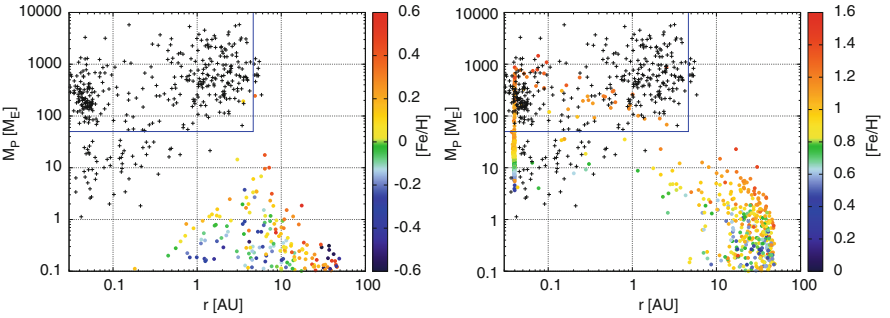

Fig. 12.10 Mass—orbital distance diagram of planetary seeds growing by planetesimal accretion, where planetary migration is completely suppressed (*left*) and in a disk where the metallicity of planetesimals is increased by a factor of 10 compared to the simulations before, but where migration is taken into account. This results in both cases in the growth of some cold gas giants compared to Fig. 12.9. Note here the different colour scales for the metallicities

grow. In the very inner regions of the disk the planetesimal isolation mass is very small, so that the planets stay below a few Earth masses. Outside of a few AU and inside of 10 AU, the planetesimal isolation mass is large enough to form cores of a few Earth masses than can accrete a gaseous envelope. However, at even larger orbital distances, the accretion rate becomes way too slow due to the low $\Sigma_{\rm pla}$, so that the planets do not grow big enough to attract a gaseous envelope.

When increasing the planetesimal surface density by a factor of 10, the growth time-scales of the planetary cores become short enough that the formation of planetary cores that can attract gaseous envelopes is possible at distances of up to a few AU. Additionally the planetesimal isolation mass increases [Eq. (12.8)], allowing the formation of larger planetary cores. Nevertheless, the formation of cold gas giants is only possible when [Fe/H]>1, which is not in agreement with observations (see Fig. 12.11 and the following section). In order to form cold gas giants in the planetesimal scenario, either planetary migration has to be ignored or the metallicity has to be increased to at least ten times the solar value, which does not reflect the giant planet occurrence rate in observations (Johnson et al. 2010; Buchhave et al. 2012). We therefore find both options to form giant planets in the planetesimal accretion scenario no realistic.

This is clearly different in the pebble accretion scenario, which allows fast growth of planetary cores even at large orbital distances at solar metallicity. The formation of planetary cores at these large orbital distances of 10–20 AU allows for a population of cold gas giants, which is impossible to form in the planetesimal accretion scenario at solar metallicity. The strength of the pebble accretion scenario therefore is that growth at large orbital distances is possible, so that forming planets do not move all the way into the central star before disk dissipation.

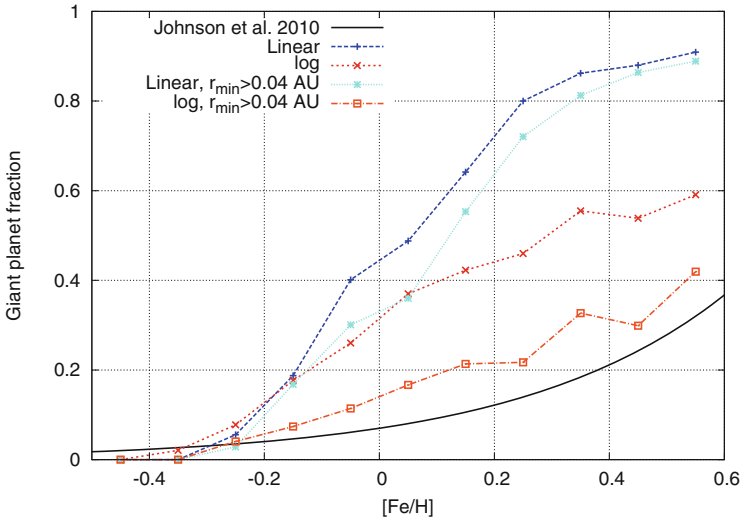

Fig. 12.11 Fraction of stars that harbour giant planets as a function of metallicity. The *black line* corresponds to Eq. (12.16) and reflects observations. The data of the simulations corresponds to the data shown in the mass-orbital distance diagrams of Figs. 12.7 and 12.8, so to planets formed in the late formation scenario. As in Johnson et al. (2010) we only take planets into account that are within 2.5 AU from the central star

12.5.5 Comparison to Observations

The strongest constraint for planet formation models is the comparison with observations. In this section we will discuss the influence of metallicity on the occurrence rate of giant planets, where we focus on the statistics obtained through RV surveys. Based on their RV measurements, Johnson et al. (2010) predict a giant planet occurrence rate around solar mass stars as a function of metallicity in the following form

$$f = 0.07 \times 10^{1.2[\mathrm{Fe/H}]}\,, \tag{12.16}$$

indicating that 7% of stars with solar metallicity ([Fe/H]=0) feature giant planets and an increasing giant planet occurrence rate with metallicity. Due to observational biases, Eq. (12.16) is only valid up to $r < 2.5$ AU, which is a different level of completeness compared to Mayor et al. (2011). We will therefore only compare our results up to this orbital distance. In Fig. 12.11 we show the fractions of stars that harbour giant planets for our simulations and compare this fraction to the observations of Johnson et al. (2010).

Our simulations follow the simplistic one-planet-per-disk approach, which only allows us to calculate the giant planet fraction by dividing the number of growth tracks that form giant planets within 2.5 AU by the total amount of planets within

the same orbital distance. This approach has several biases, because we do not take scattering of bodies into account. This is not only important at the late stages of the disk where the final system architecture is determined, but also at the early stages, where small amounts of eccentricity can significantly reduce pebble accretion (Johansen et al. 2015) and might thus hinder planetary seeds to reach pebble isolation mass and become gas giants. Therefore the results of our simulations represent a maximum giant planet fraction per planetary seed per disk. So if a disk forms e.g. 10 planetary seeds at random initial positions r_0 in a disk with [Fe/H]=0, we predict a maximum of 5 giants.

Clearly, the formation of giant planets in the pebble accretion scenario scales with increasing metallicity. An increase of metallicity allows for faster accretion rates [Eq. (12.6)], which allows to reach the pebble isolation mass at an earlier stage (Fig. 12.4), giving more time to contract the envelope around the planet and therefore results in an earlier transition to runaway gas accretion. This results in a more efficient pathway to form giant planets. In fact, it seems that the planet formation frequency is too efficient in the pebble accretion scenario.

In addition to that, the starting position of the planetary seeds plays a crucial role, because the pebble isolation mass depends on the position in the disk, where larger pebble isolation masses can be reached in the outer parts of the protoplanetary disk. In the inner parts of the disk, the pebble isolation mass is low and the formation of giant planets is not possible. This explains why the fraction of giant planets for the logarithmic starting distribution is smaller than for the linear starting distribution.

In counting the fraction of planets for $r < 2.5$ AU, we also counted the planets that reached the inner edge of the simulation at 0.04 AU. When a planet reaches this distance we stop the simulation and do not take further evolution of the planet into account. Recent simulations have shown that the atmospheres of giant planets so close to the host star can be eroded away in time (Lanza 2013), leaving only the bare planetary core behind. These giant planets would then appear as small planets in observations. The light blue and orange line in Fig. 12.11 represent the same sample of simulations, but here we counted the giant planets that reached the inner edge of the disk at 0.04 AU as small planets due to the evaporation of their atmospheres. The logarithmic starting distribution now shows only a slightly larger giant planet fraction compared to the observations of Johnson et al. (2010), where this small excess can be additionally reduced due to scattering events, which we do not take into account in our simulations.

However, we want to note here that a comparison of a one-planet-per-disk approach in our simulations to observations is not necessarily correct, but we have to choose this approach due to our model. In reality, planetary growth most likely happens within a sea of planetesimals, where the planetesimals stir each other while accreting pebbles, so that only a few, but more than one, become dominant and form planetary systems (Levison et al. 2015). Additionally, observed planetary systems are also not systems with single planets, but contain multiple planets. Therefore, future planet population synthesis models have to take the effects of multiplicity into account, in order to achieve a better comparison with observations.

12.6 Summary

In this chapter we have combined results of planet growth via pebble and gas accretion with planetary migration and disk evolution to synthesise planet populations that we compared with observations of exoplanets. We have discussed the influence of the disk's lifetime and metallicity on the growth and migration of embedded planets and compared the pebble growth mechanism with growth of planetary cores via the accretion of only planetesimals in different disk models. We especially highlighted the interplay between planet growth and migration, which is the key to form long period gas giants.

A longer disk lifetime gives more time for the planet to grow in the disk, but also allows for more efficient planetary migration. In the inner disk, where the pebble isolation mass is low, a longer disk lifetime can trigger runaway gas accretion of cores (Fig. 12.3) and allow planets of a few Earth masses to accrete gaseous envelopes to become gas giants, if the cores are trapped in the region of outward migration. However, these planets then slowly migrate inwards in type-II migration and end up as hot Jupiters. Additionally planets that are slightly too massive to be contained in the region of outward migration migrate inwards as super-Earths. Planets that form in the outer parts of the disk, on the other hand, can then eventually reach their pebble isolation mass and become gas giants on wide orbits (Fig. 12.3).

The metallicity of the protoplanetary disk influences the growth of the planetary core by two factors. First, the growth speed accelerates with metallicity resulting in faster planetary growth, which is especially important at large orbital separations, where the growth rates might be too slow to reach pebble isolation mass for low pebble metallicities. Additionally a higher metallicity allows that the planetary core can reach a higher pebble isolation mass because the time evolving disk reduces its temperature in time. Nevertheless, pebble accretion is very robust and still allows growth at larger orbital distances, so that the formation of some cold gas giants in disks with sub solar metallicity is possible.

The final orbital position of the planets is determined by the migration rates in the disk. Low mass planets migrate generally inwards, except in regions where strong negative radial gradients of entropy are present. These strong gradients exist in the inner parts of the protoplanetary disk close to the water ice line in the disk model of Bitsch et al. (2015a), while they are absent in the MMSN disk. These local gradients are also dependent on the metallicity in dust grains in the disk, which determines the cooling rates, resulting in smaller regions of outward migration in disks with low metallicity (Bitsch et al. 2015a). Additionally, the migration speed in type-I migration scales with the surface density of the protoplanetary disk. As the MMSN disk has a much higher surface density in the inner regions of the disk, planets migrate faster in that disk. The result is that all the small mass planets migrate towards the inner edge of the disk in the MMSN disk (Fig. 12.5), in contrast the planets synthesised with the (Bitsch et al. 2015a) disk, where small mass planets can stay at a distance of a few AU.

The gas accretion rate is also a function of the local surface density, resulting in the fact that gas giants in the inner parts of the disk become more massive in the MMSN disk. In fact the planets become a factor of 10 or more too massive to resemble the observed mass distribution of hot Jupiters (Fig. 12.5). For planets formed in the (Bitsch et al. 2015a) disk model, the synthesised hot Jupiters are still too massive, but much less so compared to the MMSN disk model (Fig. 12.6). This is caused when the planetary seeds form early in the disk and can thus accrete for a longer time.

As the planetesimals born from the streaming instability are a significantly smaller than the pebble transition mass [Eq. (12.4)], the planetesimals first accrete in the inefficient Bondi accretion branch to reach pebble isolation mass within about 1–1.5 Myr (Lambrechts and Johansen 2012), which we do not take into account here. We therefore invoke that the planetary seeds (at pebble transition mass) start in disks that are at least 1.5 Myr old. As a consequence, the final mass of the giant planets is smaller than for planetary seeds that start early in the disk's lifetime (Fig. 12.7), which gives a much better match to the population of hot and cold Jupiters. Additionally slightly higher masses for the synthesised super-Earth population can be achieved, matching the observations quite well.

Planetesimal accretion, on the other hand, fails completely to produce gas giants at orbits outside of 1 AU. This is caused by the long growth time-scales of the planetary cores combined with the fast migration rates. Giant planets can only emerge in those disks, when migration is unrealistically turned off or when the metallicity is increased by a factor of 10 compared to solar value (Fig. 12.10). Both options seem unrealistic.

The pebble accretion scenario confirms the metallicities trend found in observations, where the fraction of giant planets increases with stellar metallicity (Fig. 12.11). In fact, the pebble accretion scenario is very efficient in the production of giant planets and overestimates the observations by Johnson et al. (2010). This can be due to several reasons: (1) we do not take multiplicity into account which can lead to competition between the different cores for the building blocks of the planet and scattering events that will then prevent planetary growth and (2) photoevaporation of planetary atmospheres close to the central star, which can transform hot Jupiters into planetary cores due to the complete loss of the planetary envelope (Lanza 2013).

In summary, pebble accretion can explain the formation of hot and cold gas giants, as well as of super-Earths in contrast to planetesimal accretion. However, in most of the simulations the final mass of the super-Earths is a bit too small compared to the RV data. Also considering the amount of super Earths planets found by the Kepler mission, the reproduction of super-Earths in our simulations can still be improved. This may be caused by the fact that we just evolve single planet systems, while hot super-Earth systems normally feature several planets, where mutual interactions play important roles. Future population synthesis simulations therefore have to combine pebble accretion with N-body dynamics in evolving protoplanetary disks in order to constrain planet formation theories even further.

Acknowledgements B.B. and A.J. thank the Knut and Alice Wallenberg Foundation for their financial support. A.J. was also supported by the European Research Council (ERC Starting Grant 278675-PEBBLE2PLANET) and the Swedish Research Council (grant 2014-5775).

References

Alibert, Y., Mordasini, C., Benz, W.: Migration and giant planet formation. Astron. Astrophys. **417**, L25–L28 (2004)

Baillié, K., Charnoz, S., Pantin, É.: Time evolution of snow regions and planet traps in an evolving protoplanetary disk (2015). astro-phEP p arXiv:1603.07674

Baruteau, C., Crida, A., Paardekooper, S.J., Masset, F., Guilet, J., Bitsch, B., Nelson, R., Kley, W., Papaloizou, J.C.B.: Planet-disc interactions and early evolution of planetary systems. In: Protostars and Planets VI. University of Arizona Press, Tuscon (2014). arXiv:1312.4293

Birnstiel, T., Ormel, C.W., Dullemond, C.P.: Dust size distributions in coagulation/fragmentation equilibrium: numerical solutions and analytical fits. Astron. Astrophys. **525**, A11 (2011)

Birnstiel, T., Klahr, H., Ercolano, B.: A simple model for the evolution of the dust population in protoplanetary disks. Astron. Astrophys. **539**, A148 (2012)

Bitsch, B., Johansen, A.: Influence of the water content in protoplanetary discs on planet migration and formation. Astron. Astrophys. **590**, A101 (2016)

Bitsch, B., Kley, W.: Orbital evolution of eccentric planets in radiative discs. Astron. Astrophys. **523**, A30 (2010). doi:10.1051/0004-6361, 1008.2656v1

Bitsch, B., Kley, W.: Evolution of inclined planets in three-dimensional radiative discs. Astron. Astrophys. **530**, A41 (2011a)

Bitsch, B., Kley, W.: Range of outward migration and influence of the disc's mass on the migration of giant planet cores. Astron. Astrophys. **536**, A77 (2011b)

Bitsch, B., Crida, A., Morbidelli, A., Kley, W., Dobbs-Dixon, I.: Stellar irradiated discs and implications on migration of embedded planets I: equilibrium discs. Astron. Astrophys. **549**, A124 (2013)

Bitsch, B., Morbidelli, A., Lega, E., Crida, A.: Stellar irradiated discs and implications on migration of embedded planets II: accreting-discs. Astron. Astrophys. **564**, A135 (2014)

Bitsch, B., Johansen, A., Lambrechts, M., Morbidelli, A.: The structure of protoplanetary discs around evolving young stars. Astron. Astrophys. **575**, A28 (2015a)

Bitsch, B., Lambrechts, M., Johansen, A.: The growth of planets by pebble accretion in evolving protoplanetary discs. Astron. Astrophys. **582**, A112 (2015b)

Brauer, F., Henning, T., Dullemond, C.P.: Planetesimal formation near the snow line in MRI-driven turbulent protoplanetary disks. Astron. Astrophys. **487**, L1–L4 (2008)

Buchhave, L.A., Latham, D.W., Johansen, A., Bizzarro, M., Torres, G., Rowe, J.F., Batalha, N.M., Borucki, W.J., Brugamyer, E., Cladwell, C., Bryson, S.T., Ciardi, D.R., Cochran, W.D., Endl, M., Esquerdo, G.A., Ford, E.B., Geary, J.C., Gilliland, R.L., Hansen, T., Isaacson, H., et al.: An abundance of small exoplanets around stars with a wide range of metallicities. Nature **486**, 375–377 (2012)

Coleman, G., Nelson, R.P.: Giant planet formation in radially structured protoplanetary discs (2016). astro-phEP p 1604.05191

Crida, A., Bitsch, B.: Runaway gas accretion and gap opening versus type I migration (2016). astro-phEP p arXiv:1610.05403

Dittkrist, K.M., Mordasini, C., Klahr, H., Alibert, Y., Henning, T.: Impacts of planet migration models on planetary populations. Effects of saturation, cooling and stellar irradiation. Astron. Astrophys. **567**, A121 (2014)

Dürmann, C., Kley, W.: Migration of massive planets in accreting disks. Astron. Astrophys. **574**, A52 (2015)

Dürmann, C., Kley, W.: The accretion of migrating giant planets (2016). astro-phEP p arXiv:1611.01070
Fischer, D.A., Valenti, J.: The planet-metallicity correlation. Astrophys. J. **622**, 1102–1117 (2005)
Fressin, F., Torres, G., Charbonneau, D., Bryson, S.T., Christiansen, J., Dressing, C.D., Jenkins, J.M., Walkowicz, L.M., Batalha, N.M.: The false positive rate of Kepler and the occurrence of planets. Astrophys. J. **766**, 81 (2013)
Greenberg, R., Bottke, W.F., Carusi, A., Valsecchi, G.B.: Planetary accretion rates - analytical derivation. Icarus **94**, 98–111 (1991)
Hayashi, C.: Structure of the solar nebula, growth and decay of magnetic fields and effects of magnetic and turbulent viscosities on the nebula. Prog. Theor. Phys. Suppl. **70**, 35–53 (1981)
Ida, S., Lin, D.N.C.: Toward a deterministic model of planetary formation. I. A desert in the mass and semimajor axis distributions of extrasolar planets. Astrophys. J. **604**, 388–413 (2004)
Johansen, A., Youdin, A.: Protoplanetary disk turbulence driven by the streaming instability: nonlinear saturation and particle concentration. Astrophys. J. **662**, 627–641 (2007)
Johansen, A., Mac Low, M.M., Lacerda, P., Bizzarro, M.: Growth of asteroids, planetary embryos and kuiper belt objects by chondrule accretion. Sci. Adv. **1**(3), 1500109 (2015)
Johnson, J.A., Aller, K.M., Howard, A.W., Crepp, J.R.: Giant planet occurrence in the stellar mass-metallicity plane. Publ. Astron. Soc. Pac. **122**(894), 905–915 (2010)
Kley, W., Crida, A.: Migration of protoplanets in radiative discs. Astron. Astrophys. **487**, L9–L12 (2008). doi:10.1051/0004-6361:200810033
Kley, W., Bitsch, B., Klahr, H.: Planet migration in three-dimensional radiative discs. Astron. Astrophys. **506**, 971–987 (2009). doi:10.1051/0004-6361, 0908.1863
Kokubo, E., Ida, S.: Formation of protoplanet systems and diversity of planetary systems. Astrophys. J. **581**, 666–680 (2002)
Lambrechts, M., Johansen, A.: Rapid growth of gas-giant cores by pebble accretion. Astron. Astrophys. **544**, A32 (2012)
Lambrechts, M., Johansen, A.: Forming the cores of giant planets from the radial pebble flux in protoplanetary discs. Astron. Astrophys. **572**, A107 (2014)
Lambrechts, M., Johansen, A., Morbidelli, A.: Separating gas-giant and ice-giant planets by halting pebble accretion. Astron. Astrophys. **572**, A35 (2014)
Lanza, A.F.: Star-planet magnetic interaction and evaporation of planetary atmospheres. Astron. Astrophys. **557**, A31 (2013)
Lega, E., Crida, A., Bitsch, B., Morbidelli, A.: Migration of Earth-size planets in 3D radiative discs. Mon. Not. R. Astron. Soc. **440**, 683–695 (2014)
Lega, E., Morbidelli, A., Bitsch, B., Crida, A., Szulágyi, J.: Outward Migration of planets in stellar irradiated 3D discs (2015). astro-phEP p 1506.07348
Levison, H.F., Thommes, E., Duncan, M.J.: Modeling the formation of giant planet cores. I. Evaluating key processes. Astron. J. **139**, 1297–1314 (2010)
Levison, H.F., Kretke, K., Duncan, M.J.: Growing the gas-giant planets by the gradual accumulation of pebbles. Nature **524**, 322–324 (2015)
Machida, M.N., Kokubo, E., Inutsuka, S.I., Matsumoto, T.: Gas accretion onto a protoplanet and formation of a gas giant planet. Mon. Not. R. Astron. Soc. **405**, 1227–1243 (2010)
Mamajek, E.E.: Initial conditions of planet formation: lifetimes of primordial disks. AIP Conf. Proc. **1158**, 3–10 (2009)
Mayor, M., Queloz, D.: A Jupiter-mass companion to a solar-type star. Nature **378**, 355–359 (1995)
Mayor, M., Marmier, M., Lovis, C., Udry, S., Segransan, D., Pepe, F., Benz, W., Bertaux, J.L., Bouchy, F., Dumusque, X., Lo Curto, G., Mordasini, C., Queloz, D., Santos, N.C.: The HARPS search for southern extra-solar planets XXXIV. Occurrence, mass distribution and orbital properties of super-Earths and Neptune-mass planets (2011). astro-phEP p arXiv:1109.2497
Mizuno, H.: Formation of the giant planets. Prog. Theor. Phys. **64**, 544–557 (1980)
Morbidelli, A., Lambrechts, M., Jacobson, S.A., Bitsch, B.: The great dichotomy of the Solar System: small terrestrial embryos and massive giant planet cores (2015). astro-phEP p arXiv:1506.01666

Ogihara, M., Morbidelli, A., Guillot, T.: A reassessment of the in situ formation of close-in super-Earths. Astron. Astrophys. **578**, A36 (2015)

Ormel, C.W., Klahr, H.H.: The effect of gas drag on the growth of protoplanets. Analytical expressions for the accretion of small bodies in laminar disks. Astron. Astrophys. **520**, A43 (2010)

Paardekooper, S.J., Mellema, G.: Halting type I planet migration in non-isothermal disks. Astron. Astrophys. **459**, L17–L20 (2006). doi:10.1051/0004-6361:20066304, arXiv:astro-ph/0608658

Paardekooper, S.J., Baruteau, C., Kley, W.: A torque formula for non-isothermal Type I planetary migration - II. Effects of diffusion. Mon. Not. R. Astron. Soc. **410**, 293–303 (2011)

Piso, A.M.A., Youdin, A.: On the minimum core mass for giant planet formation at wide separations. Astrophys. J. **786**, 21 (2014)

Pollack, J.B., Hubickyj, O., Bodenheimer, P., Lissauer, J.J., Podolak, M., Greenzweig, Y.: Formation of the giant planets by concurrent accretion of solids and gas. Icarus **124**, 62–85 (1996)

Raettig, N., Klahr, H.H., Lyra, W.: Particle trapping and streaming instability in vortices (2015). astro-phEP p 1501.05364

Raymond, S.N., Kokubo, E., Morbidelli, A., Morishima, R., Walsh, K.J.: Terrestrial planet formation at home and abroad. In: Protostars and Planets VI, pp. 595–618. University of Arizona Press, Tucson (2014)

Ros, K., Johansen, A.: Ice condensation as a planet formation mechanism. Astron. Astrophys. **552**, A137 (2013)

Safronov, V: Evoliutsiia doplanetnogo oblaka (1969)

Tanaka, H., Ida, S.: Growth of a migrating protoplanet. Icarus **139**, 350–366 (1999)

Tanaka, H., Takeuchi, T., Ward, W.R.: Three-dimensional interaction between a planet and an isothermal gaseous disk. I. Corotation and lindblad torques and planet migration. Astrophys. J. **565**, 1257–1274 (2002)

Ward, W.R.: Protoplanet migration by nebula tides. Icarus **126**, 261–281 (1997)

Weidenschilling, S.J.: Aerodynamics of solid bodies in the solar nebula. Mon. Not. R. Astron. Soc. **180**, 57–70 (1977)

Weidenschilling, S.J.: The distribution of mass in the planetary system and solar nebula. Astrophys. Space Sci. **51**, 153–158 (1977)

Youdin, A., Goodman, J.: Streaming instabilities in protoplanetary disks. Astrophys. J. **620**, 459–469 (2005)

Zsom, A., Ormel, C.W., Güttler, C., Blum, J., Dullemond, C.P.: The outcome of protoplanetary dust growth: pebbles, boulders, or planetesimals? II. Introducing the bouncing barrier. Astron. Astrophys. **513**, A57 (2010)